Nanoscale

Uptake and stability of DNA nanostructures in cells: A cross-sectional overview of the current state of the art

Journal:	*Nanoscale*
Manuscript ID	NR-MRV-10-2022-005868.R1
Article Type:	Minireview
Date Submitted by the Author:	12-Dec-2022
Complete List of Authors:	Mathur, Divita; Case Western Reserve University, Chemistry Galvan, Angelica; US Naval Research Laboratory; University of Maryland at College Park Green, Christopher; US Naval Research Laboratory, Center for Bio/Molecular Science and Engineering, Code 6900 Liu, Kevin; Case Western Reserve University, Chemistry Medintz, Igor; U.S. Naval Research Laboratory, Center for Bio/Molecular Science and Engineering

ARTICLE

Uptake and stability of DNA nanostructures in cells: A cross-sectional overview of the current state of the art

Received 00th January 20xx,
Accepted 00th January 20xx

DOI: 10.1039/x0xx00000x

Divita Mathur,*[a] Angelica R. Galvan, [b,c] Christopher M. Green,[c] Kevin Liu,[a] and Igor L. Medintz [c]

The physical and chemical properties of synthetic DNA have transformed this prototypical biopolymer into a versatile nanoscale building block material in the form of DNA nanotechnology. DNA nanotechnology is, in turn, providing unprecedented precision bioengineering for numerous biomedical applications at the nanoscale including next generation immune-modulatory materials, vectors for targeted delivery of nucleic acids, drugs, and contrast agents, intelligent sensors for diagnostics, and theranostics, which combines several of these functionalities into a single construct. Assembling a DNA nanostructure to be programmed with a specific number of targeting moieties on its surface to imbue it with concomitant cellular uptake and retention capabilities along with carrying a specific therapeutic dose is now eminently feasible due to the extraordinary self-assembling properties and high formation efficiency of these materials. However, what remains still only partially addressed is how exactly this class of materials is taken up into cells in both the native state and as targeted or chemically facilitated along with how stable they are inside the cellular cytosol and other cellular organelles. In this minireview, we summarize what is currently reported in the literature about how (i) DNA nanostructures are taken up into cells along with (ii) what is understood about their subsequent stability in the complex multi-organelle environment of the cellular milieu along with biological fluids in general. This allows us to highlight the many challenges that still remain to overcome in understanding DNA nanostructure-cellular interactions in order to fully translate these exciting new materials.

Introduction

The importance of formulating a predictable relationship between the properties of DNA nanostructures (DNA NS or NS) and their structural integrity along with their intracellular behavior is emphasized in their now frequently demonstrated potential as designer nanoscale platforms for targeted medical interventions.[1-4] DNA NS have shown potential superiority in delivering pharmaco-chemical or nucleic acid therapeutics against several diseases as compared to current drugs. The targeted delivery of chemotherapeutic drugs *via* DNA NS in comparison to direct intravenous administration can dramatically reduce off-target toxicity.[5-8] Their versatility is highlighted by examples where thrombin-DNA aptamer chemistry has been leveraged in DNA platforms to, on one hand, induce targeted damage in the vasculature of tumor sites in Chinese hamster animal models[9] and, on the other hand, prevent thrombosis during hemodialysis by sequestering protein activity from plasma.[10, 11] In another example of this material's versatility, RNA-targeting protein RNAse A bound to DNA platforms *via* sulfo-SMCC protein-DNA chemistry was able to induce cell death in cancer MCF-7 cells.[12] Optimizing the display of ligands,[13-16] aptamers,[17-19] and antigens[20, 21] on the NS surface to match the spatial pattern of membrane receptors improves the therapeutic efficacy, particularly the B-cell recognition, of engineered DNA NS as vaccines,[19, 20] cancer treatment, or immunogenic treatments. In addition to interfacing with cells, DNA NS can potentially be programmed to remain inactive until the right biological signal stimulates a mechano-chemical actuation; these cues can include that originating from light-induced antigen binding,[22] aptamer-protein binding,[9, 23] antigen-ligand binding,[24] and many others that are yet to be incorporated into prototypical biomedical systems.[25, 26] Combining imaging with therapeutic application is also possible due to the multiplexed functionality of DNA nanoparticles.[27] Alongside performing the aforementioned delivery functionalities, the off-target immune response elicited by DNA NS is often low up to considerably high doses.[28] Most excitingly, delivering genes for Cas9-mediated genome integration is possible using the superior structural properties of DNA NS.[29]

As synthetic DNA-based therapeutic NS mature and start being prototyped for the aforementioned applications, confident prediction of the stability and structural integrity of a DNA NS inside the body at any point in time persists as a significant challenge. There are general observations that suggest that, depending on the structural and/or functional "complexity" of a DNA NS, it could remain "stable" up to a certain number of hours within the extracellular environment, serum, blood, and the cytosol (*vide infra*). Whole animal delivery studies show that the shape of a DNA NS imparts certain renal targeting advantages over unfolded plasmid

[a] *Department of Chemistry, Case Western Reserve University, Cleveland OH 44106, USA.*
[b] *Fischell Department of Bioengineering, University of Maryland, College Park MD 20742, USA.*
[c] *Center for Bio/Molecular Science and Engineering, Code 6900, US Naval Research Laboratory, Washington DC 20375, USA.*
*Correspondence: divita.mathur@case.edu

DNA which can be leveraged for renal intervention.[30] Collectively processing such observations to formulate a framework that could guide future design criteria has yet to be done and this is something that is crucial prior to clinical trial scrutiny.

The complexity of the journey that a DNA NS will undergo for delivery into a cell should be appreciated. Using the context of targeting a solid tumor in an animal model as a descriptive model, the NS will most likely be first administered as a bolus or by slower infusion in the blood stream, intramuscularly, to the lymphatic system, or even in a transdermal manner. Assuming a targeting moiety is attached to the NS, such as an arginylglycylaspartic acid (RGD) peptide motif or folic acid targeting tumors displaying integrin or folic acid receptors, respectively, the NS will then selectively bind to the tumor cell surfaces.[31] The DNA NS then are usually taken up into the cells by some form of endocytosis that in this case is most likely receptor mediated, but which for untargeted NS may be a more non-specific mechanism, these are reviewed in refs.[2, 32] Now once inside the endolysosomal system and entrapped in endosomal vesicles, the DNA NS need to escape this harsh environment to access the cytosol and subsequently enter the nucleus or mitochondria if those organelles are the required targets of the intervention. **Figure 1** provides an excellent overview of the interactions occurring during the endocytic uptake of a DNA nanorod into H1299 (transformed lung carcinoma epithelial) cells as followed by transmission electron microscopy (TEM), which, in this case, also shows the hydrolysis of the structure after being present in acidic lysosomes over 24 h.[33] Suffice to say that DNA NS have already been shown to discreetly access these different components of a mammalian cell - they can robustly match the spatial pattern and maximize their interaction with membrane receptors,[20, 21] undergo endocytosis to access intracellular space,[34, 35] and make deliveries into the cytosol and even the nucleus.[12, 35] How one DNA NS accomplishes all this while another different assembly architecture does not, how they can be engineered specifically enough, and the fundamental rules that determine a given intracellular pathway remain poorly understood.

Herein, a progress report consolidating the knowledge gained so far in elucidating the uptake mechanisms and stability of DNA NS in cellular and biological environments is presented. The DNA NS discussed here constitute 10-200 nanometer (nm) structures, or sometimes larger, as prepared by self-assembly of a pool of single stranded DNA (ssDNA) molecules *via* thermal annealing. DNA materials of this kind are typically designed based on two overarching strategies, namely, DNA origami[36] and complete ssDNA assembly.[37, 38] For more information on the DNA materials themselves and their properties, along with potential applications in the current context, the interested reader is referred to refs. [1, 4, 39, 40] Of particular interest are DNA NS that are examined for their innate cellular uptake abilities rather than when coupled with transfection agents[4] such as chitosan,[41] gold NPs,[42] condensing agents,[7, 43] or viral capsids.[44] These examples along with delivery of materials that are electroporated into cells, while valuable, are outside the current scope. A more extensive discussion on the *in vivo* implications of DNA NS is also reviewed recently. [1, 45] The context of interest being examined is that of understanding which properties of DNA NS facilitate interaction with the cell membrane or otherwise affect the rest of the internalization path at this stage of their development.

Uptake of DNA NS into mammalian cells

Tables 1 and 2 summarize published reports describing the state of the investigation into the uptake properties of DNA nanoparticles. **Table 1** focuses on DNA NS applied in different therapeutic contexts while **Table 2** summarizes studies geared towards fundamental understanding and typically do not contain DNA NS that were functionally modified with a drug or protein. The uptake studies listed in **Table 1** fall under the context of three overarching therapeutic applications, namely, immune-modulation, nucleic acid delivery, and pharmacochemical delivery. For each study, the type of DNA NS studied, cell type, displayed targeting moieties, dosage, and the tracked end-point are identified. Abbreviations of cell types are further defined in the table's footnotes. Predominantly, the DNA tetrahedron (~10 nm) is used in these studies but over the last several years larger DNA origami structures (~100 nm) have become more common, likely due to the availability of more sites to couple biocompatible signaling molecules. We observed that the display of targeting antigens or ligands on the surface of the DNA NS is not a requirement for uptake and that DNA NS with[21, 31, 46, 47] and without[5, 34, 48, 49] targeting moieties have been reported to be internalized by cells. The spatial arrangement of antigens on the DNA NS does, however, perform significantly better in immunostimulatory applications since it leverages B/T-cell receptor antigen pattern recognition and macrophage functionality.[20, 21, 50]

It is generally agreed that the primary mechanism of NS uptake into cells without active delivery modalities such as electroporation is almost universally that of endocytosis. Indeed, almost all the studies listed in Table 1 and Table 2 directly or indirectly align with this consensus. The most common mechanism of uptake was found to be receptor-mediated endocytosis wherein the DNA NS interact with membrane receptors and are internalized *via* endocytic vesicles (**Figure 1**). A clear uptake mechanism explaining the efficiency of internalization or the interaction of DNA NS with membrane receptors is still not fully elucidated. Colocalization of the fluorescence of dyes (typically Cyanine 5 – Cy5) coupled to DNA NS prototypes and cell lysosomal staining suggests that the structures reach the lysosomes in a NS-dependent timeframe.[51] The DNA NS in lysosomes may or may not be fully intact; some clarity is needed as to what extent the Cy5 fluorescence colocalization within lysosomes is attributed to stable DNA NS.[32, 52] Macrophage cells such as RAW264.7 (established from a tumor in a male mouse induced with the Abelson murine leukemia virus) are known to perform phagocytosis on what the human body would normally consider foreign material, but in the case of DNA NS, the distinction between

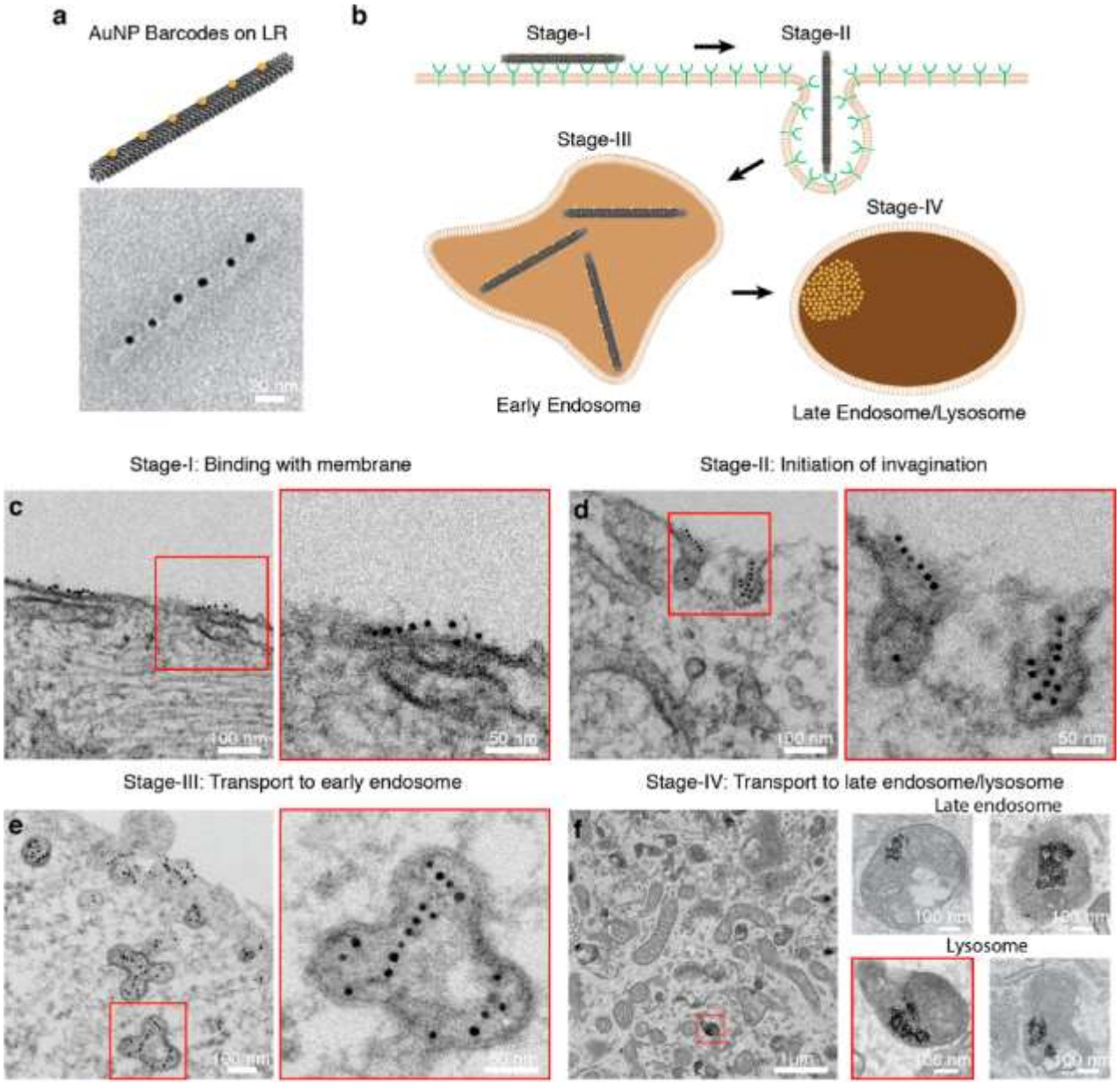

Figure 1: DNA nanoparticle endocytosis into cells. Visualization of the uptake and endocytic pathway in H1299 cells of a rod-shaped DNA nanoparticle (NP) labeled with spherical gold nanoparticles which allow for tracking via TEM imaging. (a) Schematic and representative electron microscopy image of the DNA nanorod with 6 gold nanospheres displayed along the length of the DNA nanoparticle. (b) Schematic representation of the uptake mechanism hypothesized for DNA nanorods through the four stages of endocytosis. (c-f) Step-wise representation of the transport of gold-labeled DNA nanorods from extracellular membrane to lysosomes where it can be seen that the nanorod has disintegrated (clustered instead of linearly arranged gold spheres). Reprinted (adapted) with permission from Ref. 33 Copyright 2018 American Chemical Society.

their endo- and phagocytosis and other uptake mechanisms by these cells is yet to be studied further.[50] Preliminary studies have tracked certain DNA NS in endosomes and even lysosomes of RAW264.7 cells through fluorescence colocalization studies.[21, 53]

The shape or structural complexity of DNA NS is a factor that modulates the timeframes in which the structures enter the cell and collect in the lysosomes before complete degradation.[33] While it is not immediately evident from **Tables 1 and 2** how the physicochemical properties of DNA NS determine which endocytic pathway they might trigger (since 7-400 nm large rods, tubes, polyhedral, disks, and other shapes are amenable to uptake), preliminary experimental and computational analysis suggest that the vertices of polygonal DNA NS offer the path of least resistance in terms of interfacing with the negatively charged cell membrane for endocytosis.[54, 55] More recent work by Bhatia and co-workers more systematically corroborates that tetrahedron endocytosis occurs more readily than for other larger polyhedral structures, and the size of the tetrahedral shape (14.3 nm "medium" size *versus* "large" 32 nm or "small" 11 nm) can affect its endocytic efficacy.[56] Cancerous cell lines have higher uptake propensity for DNA NS than non-cancerous. The implication of understanding the role of NS shape in

over uptake can be considered crucial to formalizing the physical factors of DNA NS that determine their cellular interaction.

Stability of DNA NS in biological environments

Over the last decade, considerable effort by the scientific community has helped decipher the preliminary structural stability of DNA nanoparticles in some extracellular *in vitro*-related environments; knowledge of this forms one of the primary barriers to the development of any translational biomedical products. These environments include cell culture media, blood serums (most commonly fetal bovine serum – FBS), and various buffers with salt and pH conditions mimicking what could be experienced *in vivo* for mammalian cells and the body, as summarized in **Tables 3 and 4**. In biological environments, the integrity of DNA NS can be rapidly compromised through attacks by various DNA nucleases (DNases), low divalent cation concentrations (common to nearly all physiological environments), and large variations in ionic strength and pH, particularly upon uptake into cells or ingestion into the stomach with its inherently acidic environment which is naturally hydrolytic.[39, 40] For eventual therapeutic applications, a DNA NS must be sufficiently robust to maintain structural integrity long enough to enter the body, travel to a target of interest, and undergo any desired interactions, such as uptake, macrophage capture, or viral capture.[57, 58] The timescales for such interactions range from minutes to tens of hours, though most applications require lifetimes on the order of several hours in the body.

In vitro studies have played a particularly outsized role in deciphering the relationship between DNA NS design and resilience in physiological environments, owing to the fine-grained control of environmental conditions that cannot be achieved *in vivo*, as well as compatibility with large, multiplexed assays that can probe many design criteria and conditions simultaneously. Studies of the resilience of DNA NS against nucleases have shown that stability varies widely depending on the physical properties of the NS, as highlighted in several recent reviews,[32, 39, 40, 59-61] and structures with greater topological complexity, helical density, and crossover density have been shown to possess greater resistance to degradation by nucleases.[62-64] Unfortunately, DNA NS with these characteristics tend to possess reduced thermal stability and require higher divalent cation concentrations to remain stable in solution. This is particularly notable in closely packed structures with high charge densities and

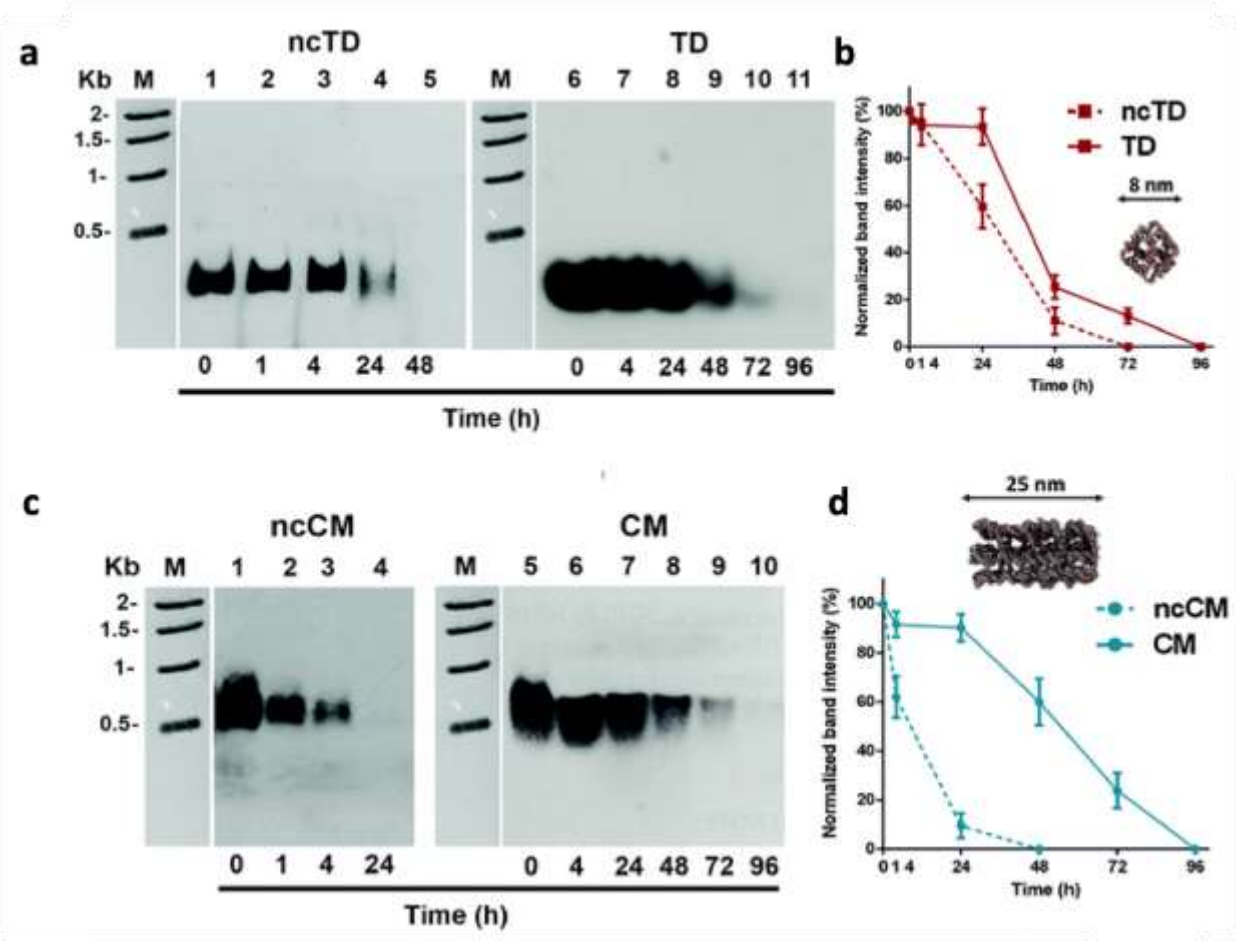

Figure 2: Stability of selected DNA NS in FBS containing serum without and with non-covalent (nc) linkage. The NS studied, namely, (a,b) Tetrahedral (TD) and (c,d) Chainmail (CM), were covalently interlocked via alkyne-azide linkage between ends of adjacent DNA molecules. Stability was studied in the presence of 10% FBS serum and measured via agarose gel electrophoresis with the results of the corresponding densitometric analysis shown in the accompanying plots. Reproduced from Ref 69 with permission from the Royal Society of Chemistry. Copyright 2019.

to a lesser extent in structures with high crossover densities, often achieved with crossovers at nonideal positions and/or by shortening the length of complementary domains in the structure.[63, 64] Despite the potential drawbacks, these modifications can improve the stability of native DNA NS in the presence of nucleases by an order of magnitude or more and are thus useful tools in the design of nuclease-resistant nanostructures.

Beyond the use of native DNA NS, many strategies to modify and/or protect DNA NS in biological environments have been successfully demonstrated, such as polymer coatings adhered to structures electrostatically or chemically,[41, 65-67] staple strand ligation and cross-linking (**Figure 2)** with chemical,[68, 69] enzymatic,[69] and photoactivated strategies,[70] incorporation of nucleic acids with nuclease-resistant backbones such as enantiomeric L-DNA,[71] phosphorothioate DNA,[72] peptide nucleic acids (PNA),[77] and various modified RNAs,[73, 74] as well as protection with hard coatings such as silica.[75, 76] Such modifications can potentially extend the lifetimes of DNA NS in biological environments beyond that achievable with native structures, often without compromising and sometimes improving thermal and low-salt stability. A recent review article by Chandrasekaran highlights several approaches to creating nuclease resistance DNA NS.[40] **Figure 2** is an example of small DNA NS that possess better serum stability when the strands are covalently linked within them *versus* when they are not.[69] From the various reports in the literature gathered here, some general trends for structures in similar environments can be identified. The lifetime of single-stranded and duplexed DNA prior to assembly into DNA NS is typically on the order of an hour or less in serum/media and 10 min or less in buffer with nucleases.[52, 67, 78] The lifetimes of native DNA NS are improved to several hours or longer in serum/media,[5, 69, 79] though native structures are often fully degraded within an hour in buffer with nucleases.[78, 80, 81] Modified DNA NS tend to have lifetimes in serum/media on the order of days and several hours in buffer with nucleases,[65, 69, 71] though some oligolysine-based coatings have been shown to extend lifetimes to days even in exposure to high nuclease concentrations.[81]

It remains a challenge to identify more than basic trends from the consolidated studies of DNA NS stability due to a general lack of standardization and best practices between studies. Studies often vary in several ways between nanostructure design, buffer conditions, nuclease activity, types of nucleases, methods of characterizing structural integrity, and reported measures of stability.[1, 32, 40, 82] This makes it extremely hard to correlate results amongst these studies. Additionally, it is not yet common practice to calibrate the enzymatic activity of nucleases in serums and buffers, which can vary with aging and handling, prior to their use,[32, 61, 79] thus it is possible for studies to report different values for stability of the same DNA NS under identical conditions. Until some form of standards are adopted, we must rely on the consistency within

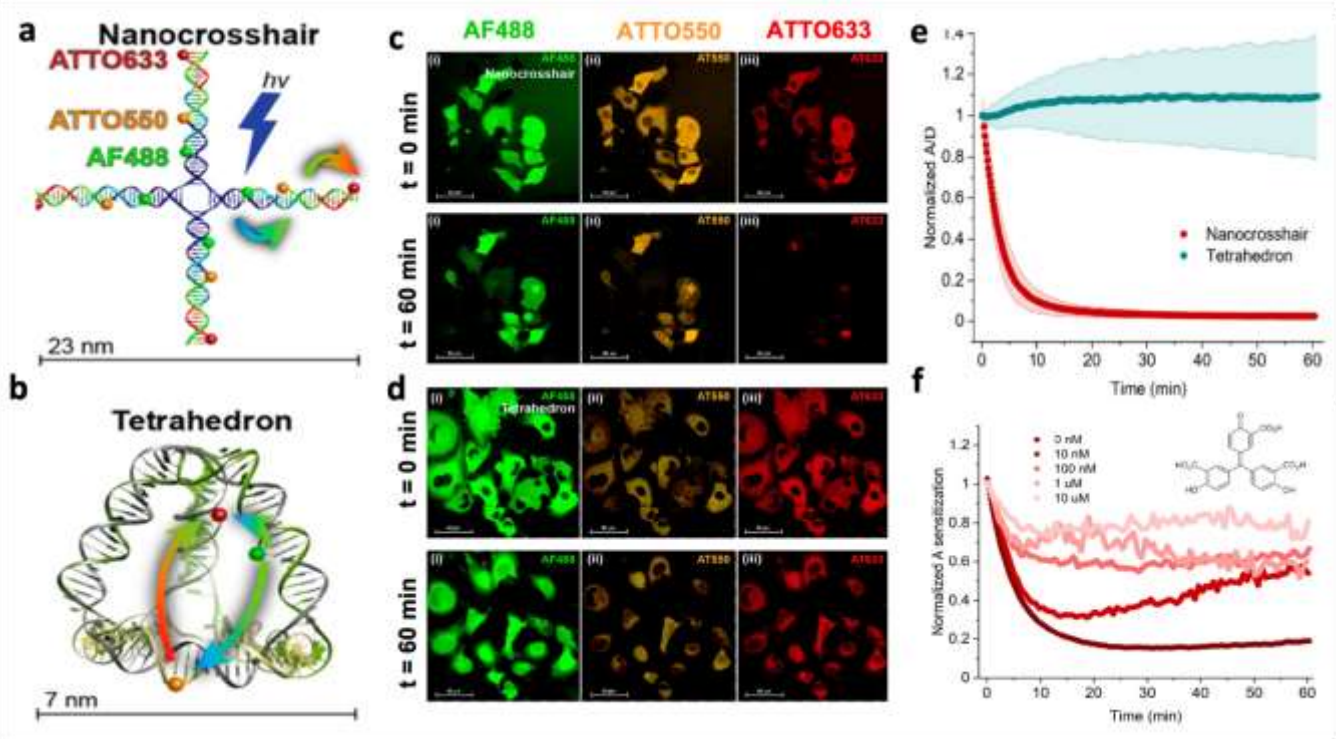

Figure 3: Schematic representing a study on the cytosolic stability of small DNA nanoparticles. Schematic with scale shown of the (a) nanocrosshair and (b) tetrahedron structures whose stability was observed directly in the cytosol of live cells. The location of dye labels and FRET pathway on each structure are also shown. COS-1 cells microinjected with the nanocrosshair (c) and (d) tetrahedron shown at t = 0 min and t = 60 min. After 60 min the FRET changed based on the change in stability of the DNA structure can be seen. (e) Plot of the change in acceptor dye to donor dye fluorescence ratio over time in the nanocrosshair *versus* tetrahedron DNA structure. (f) Plot of the change in acceptor dye to donor dye fluorescence ratio over time for microinjected samples of the nanocrosshair supplemented with the indicated concentrations of aurintricarboxylic acid nuclease inhibitor providing evidence that degradation resulted from nuclease activity. Reprinted (adapted) with permission from Ref.86 Copyright 2022 American Chemical Society.

individual studies to elucidate the preliminary rules dictating DNA NS stability in biological environments.

Conclusions and Future Outlook

From reviewing the consolidated summary of DNA NS uptake behavior (**Table 1**), it can be surmised that the overall size of the NS tested thus far ranges from a few nm (with 7 nm tetrahedron being the dominant test-bed) to 100 nm per side, which translates to an approximate range of 30 kilodaltons (kDa) up to 4 megadaltons (MDa) in terms of globular mass. The amount of different DNA NS that have been administered in uptake related studies, however, do not bear a direct correlation to NS mass, making it challenging to compare their performance in a systematic manner. This review also does not focus on the intracellular mechanisms of DNA NS endocytosis since a definitive consensus or enough data is still being sought by the field. A similar issue emerges for the stability studies highlighted in **Tables 3 and 4**, and if these issues persist, every DNA NS employed for therapeutic applications will require a case-by-case stability evaluation. It would be extremely beneficial if the field could collaborate and actively formulate a protocol for standardized quality control expected from each study that will be undertaken in the future.[83] Such assay cascades have been put into place for other nanomaterials being developed for potential clinical use.[84]

The progress in recent decades on biomedically applied DNA NS is exemplative of a promising role of the field in targeted and combinatorial therapeutic interventions. Future directions that the field has already seen some movement towards are in vaccine development through strategic antigen display or through delivery of antigenic cargo to immune cells. Combinatorial therapies, wherein adjuvants such as CpG, nanoparticles, and intercalating drugs are simultaneously delivered *via* a targeted DNA NS, are also of high interest. Lastly, delivery of functional nucleic acids through DNA NS such as silencing RNA (siRNA), or even epitope-expressing genes, warrant further investigation.

Towards achieving a status that currently favors lipid and viral-based nanoparticles as delivery systems, a few concerted efforts are needed and already underway. Consolidation into a repository of DNA NS that have been designed and engineered by the rapidly growing expert community will help repurpose successful NS in application-specific translational studies, much like the tetrahedron (originally designed by Goodman *et al.*[37]) has become prototypical in fundamental studies. Nanobase.org by Poppleton *et al.* is one such endeavor that is creating a database of DNA and RNA NS.[85] From such collaborations, one can anticipate certain DNA NS to emerge (or evolve) as superior cell- and intervention-specific (immune-stimulation *versus* nucleic acid delivery *versus* pharmacochemical delivery) options, but will more importantly be informed with recommendations on dosage, targeting moieties, and site-directed modifications by relevant studies in the literature.

The need of the hour is more cell-directed studies elucidating the programmable release and stability of DNA NS inside the cell. **Figure 3** shows results from a recent report where dye-labeled DNA structures were directly microinjected into the cytosol of a variety of different primary and transformed cells and the stability of the structures evaluated by tracking the resulting FRET over time.[86] This format was exploited to bypass the complications of endocytic uptake so that the only variable became that of cytosolic stability. This study confirmed that the high-torsion DNA tetrahedron is more stable in the cellular cytosol than linear structures. Perhaps it is worth exploring the feasibility of adopting techniques of cytosolic delivery through endocytosis that have shown promise for other non-nucleic acid nanoparticles. Like DNA NS, calcium phosphate nanoparticles (CPN) aim to be carriers that introduce medication into the cell in a noninvasive manner.[87, 88] Both nanoparticle types are taken into the cell *via* endocytosis and face stability issues as they are transported into the lysosome.[87, 88] Some stability issues can be alleviated if the CPNs can undergo endosomal escape into the cytoplasm.[87-90] Research using CPNs has shown successful endosomal escape of the nanoparticle via destabilization,[87, 88] thus we can attempt to integrate destabilizing methods, like cationic polymers[88, 89] and pH sensitive polymers[87, 89] in DNA NS administration to investigate if the same effect is observed. Furthermore, expanding cytosolic studies to other DNA NS types as well as integration of stabilizing techniques are needed.[86]

Feasibility of DNA NS based therapies on a scope where patient impact is significant are required as well. For example, to what extent are DNA NS based anti-cancer interventions advantageous from an economic standpoint is being evaluated.[91] It is also notable that the dosage of DNA NS tested in **Tables 1 and 2** are in the nM scale, urging careful evaluation of scalable synthesis needed for translating DNA NS based therapies into *in vivo* studies, let alone clinical use. Formulations testing oral or topical administration of DNA-based treatments are slowly emerging as well.[92, 93] Additionally aerosolization, lyophilized storage,[94] scalable production,[95] and long term stability[96, 97] of DNA NS have seen preliminary success in some cases but are topics in which ongoing research is actively engaged. In order to realize the widespread applicability of these fascinating materials within a medical context, everything comes back full circle to understanding their fundamental structural integrity and functional properties intracellularly and this still remains the first challenge.

Conflicts of interest

There are no conflicts to declare.

Acknowledgements

The authors acknowledge the U.S. Naval Research Laboratory (NRL), the Office of Naval Research, and the NRL's Nanoscience Institute for programmatic funding. D.M. was supported by the National Institute of Biomedical Imaging and Bioengineering of the National Institutes of Health under Award Number R00EB030013-03. The content is solely the responsibility of the authors and does not necessarily represent the official views of the National Institutes of Health.

ORCiDs:
C.M.G.: 0000-0001-7848-7144; D.M.: 0000-0002-3537-7292; I.L.M.: 0000-0002-8902-4687; A.R.G.: 0000-0002-7616-4760;

References

1. D. Mathur and I. L. Medintz, *Adv Healthc Mater*, 2019, **8**, e1801546.
2. S. Jiang, Z. Ge, S. Mou, H. Yan and C. Fan, *Chem*, 2021, **7**, 1156-1179.
3. A. H. Okholm and J. Kjems, *Expert Opin Drug Deliv*, 2017, **14**, 137-139.
4. A. Keller and V. Linko, *Angew Chem Int Ed Engl*, 2020, **59**, 15818-15833.
5. A. Udomprasert, C. Wootthichairangsan, R. Duangrat, S. Chaithongyot, Y. Zhang, R. Nixon, W. Liu, R. Wang, M. Ponglikitmongkol and T. Kangsamaksin, *ACS Appl Bio Mater*, 2022, **5**, 2262-2272.
6. Q. Jiang, C. Song, J. Nangreave, X. Liu, L. Lin, D. Qiu, Z. G. Wang, G. Zou, X. Liang, H. Yan and B. Ding, *J Am Chem Soc*, 2012, **134**, 13396-13403.
7. S. Palazzolo, M. Hadla, C. Russo Spena, I. Caligiuri, R. Rotondo, M. Adeel, V. Kumar, G. Corona, V. Canzonieri, G. Toffoli and F. Rizzolio, *Cancers (Basel)*, 2019, **11**, 1997.
8. Y. Zeng, J. Liu, S. Yang, W. Liu, L. Xu and R. Wang, *J Mater Chem B*, 2018, **6**, 1605-1612.
9. S. Li, Q. Jiang, S. Liu, Y. Zhang, Y. Tian, C. Song, J. Wang, Y. Zou, G. J. Anderson, J. Y. Han, Y. Chang, Y. Liu, C. Zhang, L. Chen, G. Zhou, G. Nie, H. Yan, B. Ding and Y. Zhao, *Nat Biotechnol*, 2018, **36**, 258-264.
10. S. Zhao, R. Tian, J. Wu, S. Liu, Y. Wang, M. Wen, Y. Shang, Q. Liu, Y. Li, Y. Guo, Z. Wang, T. Wang, Y. Zhao, H. Zhao, H. Cao, Y. Su, J. Sun, Q. Jiang and B. Ding, *Nat Commun*, 2021, **12**, 358.
11. A. Rangnekar, A. M. Zhang, S. S. Li, K. M. Bompiani, M. N. Hansen, K. V. Gothelf, B. A. Sullenger and T. H. LaBean, *Nanomedicine*, 2012, **8**, 673-681.
12. S. Zhao, F. Duan, S. Liu, T. Wu, Y. Shang, R. Tian, J. Liu, Z. G. Wang, Q. Jiang and B. Ding, *ACS Appl Mater Interfaces*, 2019, **11**, 11112-11118.
13. J. Hellmeier, R. Platzer, A. S. Eklund, T. Schlichthaerle, A. Karner, V. Motsch, M. C. Schneider, E. Kurz, V. Bamieh, M. Brameshuber, J. Preiner, R. Jungmann, H. Stockinger, G. J. Schutz, J. B. Huppa and E. Sevcsik, *Proc Natl Acad Sci U S A*, 2021, **118**, e2016857118.
14. J. Hellmeier, R. Platzer, V. Muhlgrabner, M. C. Schneider, E. Kurz, G. J. Schutz, J. B. Huppa and E. Sevcsik, *ACS Nano*, 2021, **15**, 15057-15068.
15. R. Dong, T. Aksel, W. Chan, R. N. Germain, R. D. Vale and S. M. Douglas, *Proc Natl Acad Sci U S A*, 2021, **118**, e2109057118.
16. T. Fang, J. Alvelid, J. Spratt, E. Ambrosetti, I. Testa and A. I. Teixeira, *ACS Nano*, 2021, **15**, 3441-3452.
17. Y. Sakai, M. S. Islam, M. Adamiak, S. C. Shiu, J. A. Tanner and J. G. Heddle, *Genes (Basel)*, 2018, **9**, 571.
18. Y. Wang, J. Zhu, W. Jia, H. Xiong, W. Qiu, R. Xu and Y. Lin, *ACS Appl Mater Interfaces*, 2022, **14**, 44228-44238.
19. S. Wan, S. Liu, M. Sun, J. Zhang, X. Wei, T. Song, Y. Li, X. Liu, H. Chen, C. J. Yang and Y. Song, *ACS Nano*, 2022, **16**, 15310-15317.
20. R. Veneziano, T. J. Moyer, M. B. Stone, E. C. Wamhoff, B. J. Read, S. Mukherjee, T. R. Shepherd, J. Das, W. R. Schief, D. J. Irvine and M. Bathe, *Nat Nanotechnol*, 2020, **15**, 716-723.
21. A. Comberlato, M. M. Koga, S. Nussing, I. A. Parish and M. M. C. Bastings, *Nano Lett*, 2022, **22**, 2506-2513.
22. I. Seitz, H. Ijas, V. Linko and M. A. Kostiainen, *ACS Appl Mater Interfaces*, 2022, **14**, 38515-38524.
23. S. M. Douglas, I. Bachelet and G. M. Church, *Science*, 2012, **335**, 831-834.
24. W. Engelen, C. Sigl, K. Kadletz, E. M. Willner and H. Dietz, *J Am Chem Soc*, 2021, **143**, 21630-21636.
25. P. Pitikultham, Z. Wang, Y. Wang, Y. Shang, Q. Jiang and B. Ding, *ChemMedChem*, 2022, **17**, e202100635.
26. K. E. Bujold, J. C. C. Hsu and H. F. Sleiman, *J Am Chem Soc*, 2016, **138**, 14030-14038.
27. D. Jiang, Y. Sun, J. Li, Q. Li, M. Lv, B. Zhu, T. Tian, D. Cheng, J. Xia, L. Zhang, L. Wang, Q. Huang, J. Shi and C. Fan, *ACS Appl Mater Interfaces*, 2016, **8**, 4378-4384.
28. C. R. Lucas, P. D. Halley, A. A. Chowdury, B. K. Harrington, L. Beaver, R. Lapalombella, A. J. Johnson, E. K. Hertlein, M. A. Phelps, J. C. Byrd and C. E. Castro, *Small*, 2022, **18**, e2108063.
29. E. Lin-Shiao, W. G. Pfeifer, B. R. Shy, M. Saffari Doost, E. Chen, V. S. Vykunta, J. R. Hamilton, E. C. Stahl, D. M. Lopez, C. R. Sandoval Espinoza, A. E. Deyanov, R. J. Lew, M. G. Poirer, A. Marson, C. E. Castro and J. A. Doudna, *Nucleic Acids Res*, 2022, **50**, 1256-1268.
30. D. Jiang, Z. Ge, H. J. Im, C. G. England, D. Ni, J. Hou, L. Zhang, C. J. Kutyreff, Y. Yan, Y. Liu, S. Y. Cho, J. W. Engle, J. Shi, P. Huang, C. Fan, H. Yan and W. Cai, *Nat Biomed Eng*, 2018, **2**, 865-877.
31. H. Lee, A. K. Lytton-Jean, Y. Chen, K. T. Love, A. I. Park, E. D. Karagiannis, A. Sehgal, W. Querbes, C. S. Zurenko, M. Jayaraman, C. G. Peng, K. Charisse, A. Borodovsky, M. Manoharan, J. S. Donahoe, J. Truelove, M. Nahrendorf, R. Langer and D. G. Anderson, *Nat Nanotechnol*, 2012, **7**, 389-393.
32. C. M. Green, D. Mathur and I. L. Medintz, *J Mater Chem B*, 2020, **8**, 6170-6178.
33. P. Wang, M. A. Rahman, Z. Zhao, K. Weiss, C. Zhang, Z. Chen, S. J. Hurwitz, Z. G. Chen, D. M. Shin and Y. Ke, *J Am Chem Soc*, 2018, **140**, 2478-2484.
34. G. Vindigni, S. Raniolo, A. Ottaviani, M. Falconi, O. Franch, B. R. Knudsen, A. Desideri and S. Biocca, *ACS Nano*, 2016, **10**, 5971-5979.
35. L. Liang, J. Li, Q. Li, Q. Huang, J. Shi, H. Yan and C. Fan, *Angew Chem Int Ed Engl*, 2014, **53**, 7745-7750.
36. P. W. Rothemund, *Nature*, 2006, **440**, 297-302.
37. R. P. Goodman, R. M. Berry and A. J. Turberfield, *Chem Commun (Camb)*, 2004, **12**, 1372-1373.
38. Y. Ke, L. L. Ong, W. M. Shih and P. Yin, *Science*, 2012, **338**, 1177-1183.
39. S. Manuguri, M. K. Nguyen, J. Loo, A. K. Natarajan and A. Kuzyk, *Bioconjug Chem*, 2022, DOI: 10.1021/acs.bioconjchem.2c00311.
40. A. R. Chandrasekaran, *Nat Rev Chem*, 2021, **5**, 225-239.
41. Y. Ahmadi, E. De Llano and I. Barisic, *Nanoscale*, 2018, **10**, 7494-7504.
42. S. Park and K. Hamad-Schifferli, *ACS Nano*, 2010, **4**, 2555-2560.

43. A. Chopra, S. Krishnan and F. C. Simmel, *Nano Lett*, 2016, **16**, 6683-6690.
44. J. Mikkila, A. P. Eskelinen, E. H. Niemela, V. Linko, M. J. Frilander, P. Torma and M. A. Kostiainen, *Nano Lett*, 2014, **14**, 2196-2200.
45. K. Kansara, A. Kumar and D. Bhatia, *Applied NanoMedicine*, 2022, **22**, 337.
46. M. A. Rahman, P. Wang, Z. Zhao, D. Wang, S. Nannapaneni, C. Zhang, Z. Chen, C. C. Griffith, S. J. Hurwitz, Z. G. Chen, Y. Ke and D. M. Shin, *Angew Chem Int Ed Engl*, 2020, **59**, 12575.
47. M. A. Rahman, P. Wang, Z. Zhao, D. Wang, S. Nannapaneni, C. Zhang, Z. Chen, C. C. Griffith, S. J. Hurwitz, Z. G. Chen, Y. Ke and D. M. Shin, *Angew Chem Int Ed Engl*, 2017, **56**, 16023-16027.
48. B. Smolkova, T. MacCulloch, T. F. Rockwood, M. Liu, S. J. W. Henry, A. Frtus, M. Uzhytchak, M. Lunova, M. Hof, P. Jurkiewicz, A. Dejneka, N. Stephanopoulos and O. Lunov, *ACS Appl Mater Interfaces*, 2021, **13**, 46375-46390.
49. A. S. Walsh, H. Yin, C. M. Erben, M. J. Wood and A. J. Turberfield, *ACS Nano*, 2011, **5**, 5427-5432.
50. N. Kern, R. Dong, S. M. Douglas, R. D. Vale and M. A. Morrissey, *Elife*, 2021, **10**, 68311.
51. V. Prakash, K. Tsekouras, M. Venkatachalapathy, L. Heinicke, S. Presse, N. G. Walter and Y. Krishnan, *Angew Chem Int Ed Engl*, 2019, **58**, 3073-3076.
52. A. Lacroix, E. Vengut-Climent, D. de Rochambeau and H. F. Sleiman, *ACS Cent Sci*, 2019, **5**, 882-891.
53. X. Liu, Y. Xu, T. Yu, C. Clifford, Y. Liu, H. Yan and Y. Chang, *Nano Lett*, 2012, **12**, 4254-4259.
54. H. Ding, J. Li, N. Chen, X. Hu, X. Yang, L. Guo, Q. Li, X. Zuo, L. Wang, Y. Ma and C. Fan, *ACS Cent Sci*, 2018, **4**, 1344-1351.
55. X. Peng, S. Fang, B. Ji, M. Li, J. Song, L. Qiu and W. Tan, *Nano Lett*, 2021, **21**, 6946-6951.
56. A. Rajwar, S. R. Shetty, P. Vaswani, V. Morya, A. Barai, S. Sen, M. Sonawane and D. Bhatia, *ACS Nano*, 2022, **16**, 10496-10508.
57. C. Sigl, E. M. Willner, W. Engelen, J. A. Kretzmann, K. Sachenbacher, A. Liedl, F. Kolbe, F. Wilsch, S. A. Aghvami, U. Protzer, M. F. Hagan, S. Fraden and H. Dietz, *Nat Mater*, 2021, **20**, 1281-1289.
58. S. Ren, K. Fraser, L. Kuo, N. Chauhan, A. T. Adrian, F. Zhang, R. J. Linhardt, P. S. Kwon and X. Wang, *Nat Protoc*, 2022, **17**, 282-326.
59. N. Stephanopoulos, *Chembiochem*, 2019, **20**, 2191-2197.
60. A. Lacroix and H. F. Sleiman, *ACS Nano*, 2021, **15**, 3631-3645.
61. H. Bila, E. E. Kurisinkal and M. M. C. Bastings, *Biomater Sci*, 2019, **7**, 532-541.
62. S. Goltry, N. Hallstrom, T. Clark, W. Kuang, J. Lee, C. Jorcyk, W. B. Knowlton, B. Yurke, W. L. Hughes and E. Graugnard, *Nanoscale*, 2015, **7**, 10382-10390.
63. A. R. Chandrasekaran, J. Vilcapoma, P. Dey, S. W. Wong-Deyrup, B. K. Dey and K. Halvorsen, *J Am Chem Soc*, 2020, **142**, 6814-6821.
64. Y. Xin, P. Piskunen, A. Suma, C. Li, H. Ijas, S. Ojasalo, I. Seitz, M. A. Kostiainen, G. Grundmeier, V. Linko and A. Keller, *Small*, 2022, **18**, e2107393.
65. N. Ponnuswamy, M. M. C. Bastings, B. Nathwani, J. H. Ryu, L. Y. T. Chou, M. Vinther, W. A. Li, F. M. Anastassacos, D. J. Mooney and W. M. Shih, *Nat Commun*, 2017, **8**, 15654.
66. N. P. Agarwal, M. Matthies, F. N. Gur, K. Osada and T. L. Schmidt, *Angew Chem Int Ed Engl*, 2017, **56**, 5460-5464.
67. J. W. Conway, C. K. McLaughlin, K. J. Castor and H. Sleiman, *Chem Commun (Camb)*, 2013, **49**, 1172-1174.
68. V. Cassinelli, B. Oberleitner, J. Sobotta, P. Nickels, G. Grossi, S. Kempter, T. Frischmuth, T. Liedl and A. Manetto, *Angew Chem Int Ed Engl*, 2015, **54**, 7795-7798.
69. S. Raniolo, S. Croce, R. P. Thomsen, A. H. Okholm, V. Unida, F. Iacovelli, A. Manetto, J. Kjems, A. Desideri and S. Biocca, *Nanoscale*, 2019, **11**, 10808-10818.
70. T. Gerling, M. Kube, B. Kick and H. Dietz, *Sci Adv*, 2018, **4**, eaau1157.
71. K. R. Kim, S. J. Kang, A. Y. Lee, D. Hwang, M. Park, H. Park, S. Kim, K. Hur, H. S. Chung, C. Mao and D. R. Ahn, *Biomaterials*, 2019, **195**, 1-12.
72. V. J. Schuller, S. Heidegger, N. Sandholzer, P. C. Nickels, N. A. Suhartha, S. Endres, C. Bourquin and T. Liedl, *ACS Nano*, 2011, **5**, 9696-9702.
73. C. Lin, Y. Ke, Z. Li, J. H. Wang, Y. Liu and H. Yan, *Nano Lett*, 2009, **9**, 433-436.
74. K. R. Kim, H. Y. Kim, Y. D. Lee, J. S. Ha, J. H. Kang, H. Jeong, D. Bang, Y. T. Ko, S. Kim, H. Lee and D. R. Ahn, *J Control Release*, 2016, **243**, 121-131.
75. L. Nguyen, M. Doblinger, T. Liedl and A. Heuer-Jungemann, *Angew Chem Int Ed Engl*, 2019, **58**, 912-916.
76. M.-K. Nguyen, V. H. Nguyen, A. K. Natarajan, Y. Huang, J. Ryssy, B. Shen and A. Kuzyk, *Chem Mater*, 2020, **32**, 6657-6665.
77. S. Fairweather, M. Rogers, P. Stoulig, F. O'Murphy, E. Bose, S. Tumusiime, A. Desany, M. Troisi, A. Alvarado, E. Wade, K. Cruz, K. Wlodychak and A. J. Bell, Jr., *Biophys Chem*, 2022, **289**, 106863.
78. J. W. Keum and H. Bermudez, *Chem Commun (Camb)*, 2009, **45**, 7036-7038.
79. J. Hahn, S. F. Wickham, W. M. Shih and S. D. Perrault, *ACS Nano*, 2014, **8**, 8765-8775.
80. C. E. Castro, F. Kilchherr, D. N. Kim, E. L. Shiao, T. Wauer, P. Wortmann, M. Bathe and H. Dietz, *Nat Methods*, 2011, **8**, 221-229.
81. F. M. Anastassacos, Z. Zhao, Y. Zeng and W. M. Shih, *J Am Chem Soc*, 2020, **142**, 3311-3315.
82. K. A. Afonin, M. A. Dobrovolskaia, G. Church and M. Bathe, *ACS Nano*, 2020, **14**, 9221-9227.
83. J. J. Rennick, A. P. R. Johnston and R. G. Parton, *Nat Nanotechnol*, 2021, **16**, 266-276.
84. NCI, Assay Cascade Characterization Program, https://www.cancer.gov/nano/research/ncl/assay-cascade, (accessed September 2, 2022).
85. E. Poppleton, A. Mallya, S. Dey, J. Joseph and P. Sulc, *Nucleic Acids Res*, 2022, **50**, D246-D252.
86. D. Mathur, K. E. Rogers, S. A. Diaz, M. E. Muroski, W. P. Klein, O. K. Nag, K. Lee, L. D. Field, J. B. Delehanty and I. L. Medintz, *Nano Lett*, 2022, **22**, 5037-5045.
87. A. Maitra, *Expert Rev Mol Diagn*, 2005, **5**, 893-905.
88. F. Pittella, M. Zhang, Y. Lee, H. J. Kim, T. Tockary, K. Osada, T. Ishii, K. Miyata, N. Nishiyama and K. Kataoka, *Biomaterials*, 2011, **32**, 3106-3114.
89. T. F. Martens, K. Remaut, J. Demeester, S. C. De Smedt and K. Braeckmans, *Nano Today*, 2014, **9**, 344-364.
90. D. Ma, *Nanoscale*, 2014, **6**, 6415-6425.
91. E. L. Coleridge and K. E. Dunn, *Biomed Phys Eng Express*, 2020, **6**.

92. G. Yang, H. E. Lee, S. W. Shin, S. H. Um, J. D. Lee, K.-B. Kim, H. C. Kang, Y.-Y. Cho, H. S. Lee and J. Y. Lee, *Adv Funct Mater*, 2018, **28**, 1801918.
93. M. Baig, S. Khan, M. A. Naeem, G. J. Khan and M. T. Ansari, *Biomed Pharmacother*, 2018, **97**, 1250-1258.
94. B. Zhu, Y. Zhao, J. Dai, J. Wang, S. Xing, L. Guo, N. Chen, X. Qu, L. Li, J. Shen, J. Shi, J. Li and L. Wang, *ACS Appl Mater Interfaces*, 2017, **9**, 18434-18439.
95. F. Praetorius, B. Kick, K. L. Behler, M. N. Honemann, D. Weuster-Botz and H. Dietz, *Nature*, 2017, **552**, 84-87.
96. Y. Xin, C. Kielar, S. Zhu, C. Sikeler, X. Xu, C. Moser, G. Grundmeier, T. Liedl, A. Heuer-Jungemann, D. M. Smith and A. Keller, *Small*, 2020, **16**, e1905959.
97. C. Kielar, Y. Xin, X. Xu, S. Zhu, N. Gorin, G. Grundmeier, C. Moser, D. M. Smith and A. Keller, *Molecules*, 2019, **24**, 2577.
98. S. Liu, Q. Jiang, X. Zhao, R. Zhao, Y. Wang, Y. Wang, J. Liu, Y. Shang, S. Zhao, T. Wu, Y. Zhang, G. Nie and B. Ding, *Nat Mater*, 2021, **20**, 421-430.
99. J. Li, H. Pei, B. Zhu, L. Liang, M. Wei, Y. He, N. Chen, D. Li, Q. Huang and C. Fan, *ACS Nano*, 2011, **5**, 8783-8789.
100. S. Kocabey, H. Meinl, I. S. MacPherson, V. Cassinelli, A. Manetto, S. Rothenfusser, T. Liedl and F. S. Lichtenegger, *Nanomaterials (Basel)*, 2014, **5**, 47-60.
101. K. E. Bujold, J. Fakhoury, T. G. W. Edwardson, K. M. M. Carneiro, J. N. Briard, A. G. Godin, L. Amrein, G. D. Hamblin, L. C. Panasci, P. W. Wiseman and H. F. Sleiman, *Chem. Sci.*, 2014, **5**, 2449-2455.
102. K. R. Kim, J. Kim, J. H. Back, J. E. Lee and D. R. Ahn, *ACS Nano*, 2022, **16**, 7331-7343.
103. Y. X. Zhao, A. Shaw, X. Zeng, E. Benson, A. M. Nystrom and B. Hogberg, *ACS Nano*, 2012, **6**, 8684-8691.
104. Z. Xia, P. Wang, X. Liu, T. Liu, Y. Yan, J. Yan, J. Zhong, G. Sun and D. He, *Biochemistry*, 2016, **55**, 1326-1331.
105. Y. Jiang, H. Zhou, W. Zhao and S. Zhang, *Anal Chem*, 2022, **94**, 6771-6780.
106. M. M. C. Bastings, F. M. Anastassacos, N. Ponnuswamy, F. G. Leifer, G. Cuneo, C. Lin, D. E. Ingber, J. H. Ryu and W. M. Shih, *Nano Lett*, 2018, **18**, 3557-3564.
107. C. X. Liu, B. Wang, W. P. Zhu, Y. F. Xu, Y. Y. Yang and X. H. Qian, *Angew Chem Int Ed Engl*, 2022, **61**, e202205509.
108. D. Bhatia, S. Surana, S. Chakraborty, S. P. Koushika and Y. Krishnan, *Nat Commun*, 2011, **2**, 339.
109. M. Fu, L. Dai, Q. Jiang, Y. Tang, X. Zhang, B. Ding and J. Li, *Chem Commun (Camb)*, 2016, **52**, 9240-9242.
110. K. R. Kim, Y. D. Lee, T. Lee, B. S. Kim, S. Kim and D. R. Ahn, *Biomaterials*, 2013, **34**, 5226-5235.
111. J. J. Fakhoury, C. K. McLaughlin, T. W. Edwardson, J. W. Conway and H. F. Sleiman, *Biomacromolecules*, 2014, **15**, 276-282.
112. S. Ramakrishnan, L. Scharfen, K. Hunold, S. Fricke, G. Grundmeier, M. Schlierf, A. Keller and G. Krainer, *Nanoscale*, 2019, **11**, 16270-16276.
113. Q. Mei, X. Wei, F. Su, Y. Liu, C. Youngbull, R. Johnson, S. Lindsay, H. Yan and D. Meldrum, *Nano Lett*, 2011, **11**, 1477-1482.

.

ARTICLE

Table 1: Overview of application-specific studies reporting uptake of DNA nanostructure by mammalian cell and animal models.

Application	DNA nanostructure (size nm/mass kDa)	Cell type *Primary* / transformed	Targeting moiety on DNA / Drug or Protein	Dosage (in x10^4 cells)$^+$	Tracked end-point	Cytotoxicity$^+$	Ref. (Year)
Immune-stimulation:	Rectangle reconfigured as tube (90 nm)	*BMDC*, mice	OVA, gp100, and Adpgk peptides	2 nM in 3x	endosome		98 (2021)
	Octahedron (50 nm), Tube (400 nm/4 MDa), Nanorod (89 nm/4 MDa)	3T3, HEK-293, H441	none	1 nM in 1x	--	None > 7d	79 (2014)
	Disk (80 nm/4 MDa)	RAW264.7	CpG	10-1000 nM in 2x	endosome	None > 5h	21 (2022)
	Tetrahedron (7 nm/82 kDa)	RAW264.7	CpG	100 nM in 50x	--	None > 24h	99 (2011)
	Rectangle (90 nm/4 MDa)	RAW264.7, THP-1	IgG	1 µM DNA in 3x	--	--	50 (2021)
	Tube (80 nm/4 MDa)	*splenic macrophages*	CpG, CpG PTO, CpG chimera	2.4 nM 50 µL DNA in 40x	lysosomes	None > 18h	72 (2011)
	Tetrahedron (7 nm/82 kDa)	RAW 264.7, *primary dendritic cells*	CpG, streptavidin	62.5 nM in 2.5x-25x	lysosomes	--	53 (2021)
Nucleic acid delivery:	Tetrahedron (7 nm/82 kDa)	HeLa	siRNA	10-80 nM in 15x	--	None > 24h	31 (2012)
	Tube (27 nm/140 kDa)	HeLa	none	10 nM	endosome	None > 24h	100 (2014)
	Rectangular prism (10 nm/160 kDa)	HeLa	DNA trigger strand	75 nM in 1x	--	None > 72h	26 (2016)
	Cube (7 nm/82 kDa)	HeLa, *primary B-lymphocytes*	DNA trigger strand	250 pmoles in 10x	--	--	101 (2014)
	Rectangle, tube (32 nm - 64 nm)	DMS53, NSCLC	siRNA	16.7 nM in 1x	cytoplasm	None > 8h	46, 47 (2020)
	Tetrahedron (7 nm/82 kDa)	Mice	SARS-CoV-2 aptamer	500 nM 100 µL inj.	--	None > 12h	19 (2022)
	Tetrahedron (7 nm/82 kDa)	Mice	TGF-β1 mRNA	1µM 200 µL inj.	Liver targeting	None > 24h	102 (2022)
	Tetrahedron (7 nm/82 kDa)	Mice	BACE1 aptamer	1 µM 100 µL inj.	cross BBB	--	18 (2022)
Pharmaco-chemical/drug:	Triangle (120 nm), rod (400 nm)	MCF-7	None / DOX	50-100 µM	--	None > 48h	6 (2012)
	Disk (62 nm/4 MDa), Donut (44 nm/4 MDa), Sphere (62 nm/4 MDa)	MCF-7, MDA-MB-231	MUC1 aptamer / DOX	1 nM in 0.3x	--	None > 48h	5 (2022)
	Cross, Rectangle, Triangle (50 nm/4 MDa)	MDA-MB-231	None / DOX	1.25 - 5 nM in 0.3x	lysosomes	--	8 (2018)

	T-nanotube, S-nanotube (100 nm/4 MDa)	MDA-MB-231, MDA-MB-468, and MCF-7	None / DOX	50 - 15000 nM Dox in 20x	endosomes	--	103 (2012)
	Tetrahedron (7 nm/82 kDa)	U87MG	tumor penetrating peptide / DOX	50 nM in 0.4x	--	--	104 (2016)
	3D DNA NS (100 nm	MCF-7, mice	MUC1 aptamer	4 μM in 10x	--	--	105 (2022)
Protein delivery:	Rectangle reconfigured as a tube (90 nm/4 MDa)	*HUVEC*, mice	AS1411 aptamer / Thrombin		--	None > 72h	9 (2018)
	Rectangle (90 nm/4 MDa)	MCF-7	MUC1 aptamer / RnaseA	1 nM	--	None > 48h	12 (2019)

Abbreviations: Adpgk = neoantigen peptide derived from MC-38 colon carcinoma, CpG = unmethylated cytosine–guanine dinucleotide motifs, DOX = doxorubicin, gp100 = peptide vaccine from melanoma antigen glycoprotein, MUC1 = Mucin 1 protein overexpressed in malignant cells, OVA = ovalbumin peptide epitope presented by class I major histocompatibility complex, PTO = kinase substrate, siRNA = small interfering RNA, inj = tail vein injection, BBB = Blood Brain Barrier.

Cell types: BMDC = bone marrow derived dendritic cells; COS = monkey kidney fibroblast cells; DMS53 = human small cell lung cancer cells; H1299 = human non-small cell lung cancer cells; H441 = human distal lung epithelial cells; HEK293 = human embryonic epithelial kidney cells; HeLa = human cervical cancer cells; Huh7 = human epithelial cancer cells; HUVEC = human umbilical vein endothelial cells; MCF-7 = human breast cancer cells; MDA-MB = human epithelial breast cancer cells; NSCLC = human non-small cell lung cancer cells; NIH-3T3 = mouse embryonic fibroblast cells; RAW264.7 = mouse macrophage cells; THP-1 = human leukemia monocytic cells; U87MG = human glioblastoma.

[+]dosage is given as $x10^4$ cells. For example, first entry represents $3x10^4$ cells.

[++]Cytotoxicity in the presence of bare DNA NS only (not the treatment in some cases).

Table 2: Studies focused on DNA nanostructure uptake in mammalian cells.

DNA nanostructure (size nm/mass kDa)	Cell type *Primary* / transformed	Targeting moiety displayed on the DNA NS	Dosage (in x10^4 cells)[+]	Tracked end-point	Cytotoxicity[+++]	Ref. (Year)
Thin rod, Thick rod, Small ring, Large ring, Barrel, Octahedron, Block (50 nm - 400 nm/4 MDa)	*BDMC*, HEK293, *HUVEC*	none	1 nM in 10x		None > 12h	106 (2018)
Octahedron (11 nm/160 kDa)	COS fibroblasts	none	2 µg/mL in 100x	cytoplasm, endosomes	--	34 (2016)
Tetrahedral nanocage (8 nm/82 kDa), Octahedral nanocage (11 nm/180 kDa), Chainmail (25 nm/180 kDa), Square box (35 nm), Rectangle (80 nm/4 MDa)	COS-7	none	6 ug/ml in 100x	lysosomes	--	69 (2019)
Tetrahedron (7 nm/82 kDa)	HEK	none	1 µg in 30x	cytoplasm	None > 72h	49 (2019)
Cube, Tetrahedron nanocages (10 nm)	HeLa	none	150 nM	lysosome, mitochondria	--	52 (2019)
Tetrahedron (7 nm/82 kDa)	HeLa	none	150 nM		None > 3h	55 (2021)
Tetrahedron (7 nm/82 kDa)	HeLa, COS-7	none	100 nM in 8x	lysosome, nucleus	--	35 (2014)
Small tetrahedron (11 nm), Large tetrahedron (47 nm), Small rod (32 nm), large rod (127 nm)	HeLa, H1299, DMS53	none	250 nM	lysosome	None > 1h	33 (2018)
6-helix bundle (6 nm x 7 nm)	HepG2, Huh7	oligolysine	50 nM in 10x	endosome, lysosome, cytoplasm	None > 24 h	48 (2021)
Concave-DNA origami structure (34 nm/4 MDa)	Hela, HepG2, MCF-7, DC2.4	pH low insertion peptide[++]	15 nM In 10x	endoplasmic reticulum	--	107 (2022)
Icosahedron (10 nm/160 kDa)	*Caenorhabditis elegans*	10 kDa FITC-Dextran	12-15 µM	endosome	--	108 (2011)
Tube (400 nm/4 MDa)	NIH-3T3	none	10 nM	lysosome	--	109 (2013)
Tetrahedron (7 nm/82 kDa)	RAW264.7	none	10 nM in 2.5x	cytoplasm	None > 6h	110 (2009)

Cell types: BMDC = bone marrow derived dendritic cells; COS = monkey kidney fibroblast cells; DMS53 = human small cell lung cancer cells; H1299 = human non-small cell lung cancer cells; HEK293 = human embryonic epithelial kidney cells; HeLa = human cervical cancer cells; Huh7 = human epithelial cancer cells; HUVEC = human umbilical vein endothelial cells; DC2.4 = immortalized murine dendritic cells; NIH-3T3 = mouse embryonic fibroblast cells; RAW264.7 = mouse macrophage cells.

[+]dosage is given as x10^4 cells. For example, first entry represents 10x10^4 cells (or 10^5 cells).

[++]The different cells were first treated with artificial membrane receptor (AMR) that enabled uptake and targeting of the DNA NS.

[+++] Cytotoxicity in the presence of bare DNA NS only (not the treatment in some cases).

Table 3: Stability of DNA nanostructures in serum.

Environment	DNA Nanostructure	Dimensions / mass	Modifications for stability	Reported Stability	Reporting	Notes	Ref. (Year)
Media/Buffers with serum							
DMEM-Mg with 10% FBS, 37 ºC	ssDNA Tetrahedron (Tet.) Cube	63,96 nt / 24,36 kDa 7 nm / 82 kDa 7 nm / 124 kDa	+/- HEG termination 3', int., 5' Cy dyes	ssDNA $\tau_{1/2}$: 0.8-4 h Tet. $\tau_{1/2}$: 7-8 h Cube $\tau_{1/2}$: 3.5-5.5 h	PAGE denat. PAGE	Cy dye position: 3' > int > 5' HEG termination > native Tet. >> Cube > ssDNA	52(2019)
DMEM with 10% FBS, 37 ºC	Disc origami Donut origami Sphere origami	62 nm dia. / 4 MDa 44 nm dia. / 4 MDa 42 nm dia. / 4 MDa	--	Disc < 12 h Donut < 24 h Sphere < 12 h	AGE	No degradation observed.	5(2022)
RPMI with 10% FBS, 37 ºC	Octahedron origami	45 nm dia. / 4 MDa	--	< 24 h	AGE, TEM	No degradation observed.	79(2014)
DMEM with 10% FBS, 37 ºC	Triangular prism	10 nm / 160 kDa	PS	$\tau_{1/2}$: 2-7 h (decreased w/ PS)	AGE, PAGE, denat. PAGE	While PS decreased structure stability, single strand stability increased	111(2013)
10% FBS, 37 ºC	Tetrahedron (Tet.) Linear dsDNA (DS)	7 nm / 82 kDa 63 bp / 41 kDa	Enzymatic ligation	FBS: Tet. > 24 h, DS ~4 h DNase: Tet. < 10 min, DS ~ 3 min	AGE	Tet. > 3× more stable than DS	78(2009)
50% FBS, 37 ºC	Tetrahedron (Tet.) Duplex	7 nm / 82 kDa 63 bp / 41 kDa	--	Tet. < 24 h Duplex < 4 h	AGE	Tet. > 4× more stable than DS	99(2011)
DMEM with 10% FBS, 37 ºC	Triangular prism ssDNA	10 nm / 160 kDa 63 bp / 41 kDa	HEG ended DNA oligos	Prism: ~ 2 h, HEG prism: >24 h ssDNA: < 1 h, HEG ssDNA: 28 h	PAGE	HEG > 10× increased stability	67(2013)
RPMI with 10% FBS, 37 ºC	Barrel origami	60 nm dia. / 4 MDa	Oligolysine (K4-K20) PEG Oligolysine (K10:P1k-10k)	For Native/K10/K10:P5k in FBS: $\tau_{1/2}$ = 5 min/55 min/36 h	AGE, TEM	Best nuclease stability with K10:P5k	65(2017)
10% FBS, 37 ºC	Tetrahedron (Tet.) Octahedron (Oct.) Chainmail rod (CM) Rectangular origami	7 nm / 82 kDa 11 nm / 180 kDa 25 nm / 180 kDa 90 × 60 nm / 4 MDa	Enzymatic ligation (Tet., Oct.) Click-chemistry ligation (CM)	Native structures: $\tau_{1/2}$ ~12 h Ligated structures: τ1/2 ~36 h Native origami: τ1/2 ~24 h	AGE	Tet. most stable structure	69(2019)
10% FBS in TAE+Mg, 37 ºC	Pyramid Triangular prism Cube Rugby-ball	10 nm / 94 kDa 12 nm / 105 kDa 12 nm / 140 kDa 18 nm / 140 kDa	2'-Fluoro-RNA (2F) 2'-O-Methyl-RNA (2OMe) Enantiomeric L-DNA	Native structures: < 1 h 2F structures: > 24 h 2OMe structures: > 24 h L-DNA structures: > 24 h	AGE	> 24× improved stability with modified backbones	71(2019)

Abbreviations: Fetal Bovine Serum (FBS), Dulbecco's Modified Eagle Medium (DMEM), Roswell Park Memorial Institute (RPMI) medium, Tris Acetate EDTA (TAE), Agarose Gel Electrophoresis (AGE), Polyacrylamide Gel Electrophoresis (PAGE), Transmission Electron Microscopy (TEM), Hexaethylene glcol (HEG), single stranded DNA (ssDNA), phosphorothioate (PS), half-life (τ1/2), hours (h), internal (int).

Table 4: Stability of DNA NS in buffers and media, buffers with nucleases, and intra/extracellular.

Environment	DNA Nanostructure	Dimensions / mass	Modifications for stability	Reported Stability	Reporting	Notes	Ref. (Year)
Buffers and media							
1X PBS	6-HB origami	7 nm / 36 kDa	--	T_m = 51 ºC in PBS	T_m (melting temperature)	No added peptide stability	48(2021)
DMEM-Mg, 37 ºC MES buffer pH 5.5, 37 ºC	Disk origami	60 nm dia. / 4.5 MDa	--	DMEM: > 5 h MES: > 5 h	AGE	No serum or nucleases	21(2022)
RPMI media low Mg, 37 ºC 5 mM Tris with 1 mM EDTA, 37 ºC	Barrel origami (x4) Block origami 24/6-HB origami Octahedron origami	30-90 nm dia./ 4 MDa 50 nm / 4 MDa 100-400 nm / 4 MDa 60 nm dia. / 4 MDa	Oligolysine (K4-K20) PEG oligolysine Spermidine, Spermine Polyethylenimine (PEI) Oligoarginine (R6)	All but PEI stabilized Structures in RPMI PEI compromised structures R6 compromised shape	AGE, TEM	Best salt stability with K6 All oligolysines stabilized all structures	65(2017)
6M urea, 23 - 42 ºC	Triangle origami	120 nm / 4 MDa	Strand redesign Enzymatic ligation	upto 30 min	AFM	Ligation increased T_m by 8 ºC	112(2019)
Buffers with nucleases							
1 U DNase I 10 U Endonucl. (T7, MseI) 10 U Exonucl.(T7, E.coli, lambda) All in NEBuffer 4, 37 ºC	18-HB origami 24-HB origami 32-HB origami pET24b ds plasmid	140 nm / 4 MDa 100 nm / 4 MDa 70 nm / 4 MDa 5309 bp / 3.3 MDa	--	Origami: < 1 h in DNase I Partial degradation in 1 h by T7 Exo Plasmid: < 5 min in DNase I	AGE, TEM	Origami stable in all but DNase I and T7 Exo Origami >> plasmid	80(2011)
1 U/uL DNase I, 37 ºC	Wide barrel origami Barrel origami	90 nm dia. / 4 MDa 60 nm dia. / 4 MDa	PEG oligolysine (K10P) Crosslinked K10P (xK10P)	Native: $\tau_{1/2}$ < 1 min with K10P: $\tau_{1/2}$ ~ 16 min with xK10P: $\tau_{1/2}$ ~ 66 h	AGE, TEM	K10P: ~400-fold improved xK10P: ~10^5-fold improved over native structures	81(2020)
0.2 U DNase I, 37 ºC	Tetrahedron (Tet.) Linear dsDNA (DS)	7 nm / 82 kDa 63 bp / 41 kDa	Enzymatic ligation	Tet. < 10 min, DS ~ 3 min	AGE	Tet. > 3× more stable than DS	78(2009)
RPMI with varying DNase I, 37 ºC	Barrel origami	60 nm dia. / 4 MDa	Oligolysine (K4-K20) PEG Oligolysine (K10:P1k-10k)	DNase for degradation in 1 h: 0.5 U/mL native, >500 U/mL K10:P5k	AGE, TEM	Best nuclease stability with K10:P5k	65(2017)
Intra/Extracellular							
Cell cytosol (COS-1, Fibroblasts, Astrocytes, A549, and HeLa cells)	Tetrahedron (Tet.) 4-arm crosshair (4ac)	7 nm / 82 kDa 23 nm / 104 kDa	--	Tet. > 1 h in all cell types 4ac < 15 min in HeLa cells	three-dye FRET	Tetrahedron >> crosshair	86(2022)
Cell lysate at 4 ºC, 25 ºC	Rectangle origami Triangle origami Block origami	90 × 60 nm / 4 MDa 120 nm / 4 MDa 30 nm / 4 MDa	--	All structures stable > 12 h	AGE, TEM, AFM	No degradation observed.	113(2011)

70% human serum, 37 ºC 97.5% whole human blood, 37 ºC	Nanotweezer (Ntw) dsDNA probe (DS) ssDNA	10 nm / 53 kDa 22 bp / 17 kDa 32 nt / 10 kDa	--	Ntw: > 24 h in serum/blood DS: > 24 h in serum/blood ssDNA: < 2 h in serum/blood	AGE, FRET	DS more stable than Ntw	62(2015)
Flowing whole blood	Tetrahedron (Tet.) 4-arm crosshair (4ac)	7 nm / 82 kDa 23 nm / 104 kDa	--	Tet. > 1 h in all cell types 4ac < 15 min in HeLa cells	three-dye FRET	Tetrahedron >> crosshair	9(2018)